Histochem Cell Biol (2014) 141:17–31
DOI 10.1007/s00418-013-1143-4

ORIGINAL PAPER

Tissue distribution and subcellular localization of hyaluronan synthase isoenzymes

Kari Törrönen · Kaisa Nikunen · Riikka Kärnä · Markku Tammi · Raija Tammi · Kirsi Rilla

Accepted: 9 September 2013 / Published online: 22 September 2013

Abstract Hyaluronan synthases (HAS) are unique plasma membrane glycosyltransferases secreting this glycosaminoglycan directly to the extracellular space. The three HAS isoenzymes (HAS1, HAS2, and HAS3) expressed in mammalian cells differ in their enzymatic properties and regulation by external stimuli, but clearly distinct functions have not been established. To overview the expression of different HAS isoenzymes during embryonic development and their subcellular localization, we immunostained mouse embryonic samples and cultured cells with HAS antibodies, correlating their distribution to hyaluronan staining. Their subcellular localization was further studied by GFP–HAS fusion proteins. Intense hyaluronan staining was observed throughout the development in the tissues of mesodermal origin, like heart and cartilages, but also for example during the maturation of kidneys and stratified epithelia. In general, staining for one or several HASs correlated with hyaluronan staining. The staining of HAS2 was most widespread, both spatially and temporally, correlating with hyaluronan staining especially in early mesenchymal tissues and heart. While epithelial cells were mostly negative for HASs, stratified epithelia became HAS positive during differentiation. All HAS isoenzymes showed cytoplasmic immunoreactivity, both in tissue sections and cultured cells, while plasma membrane staining was also detected, often in cellular extensions. HAS1 had brightest signal in Golgi, HAS3 in Golgi and microvillous protrusions, whereas most of the endogenous HAS2 immunoreactivity was localized in the ER. This differential pattern was also observed with transfected GFP–HASs. The large proportion of intracellular HASs suggests that HAS forms a reserve that is transported to the plasma membrane for rapid activation of hyaluronan synthesis.

Keywords Hyaluronan · Hyaluronan synthase · Embryonic development · Immunohistochemistry

K. Törrönen · K. Nikunen · R. Kärnä · M. Tammi · R. Tammi · K. Rilla (✉)
Institute of Biomedicine, Anatomy, University of Eastern Finland, P.O.B. 1627, 70211 Kuopio, Finland
e-mail: kirsi.rilla@uef.fi

Introduction

Hyaluronan is the largest and one of the most abundant glycosaminoglycans of the extracellular space. The way it is synthesized is unique and different from any other known mammalian glycoconjugate. Hyaluronan synthases (HASs) are glycosyltransferases acting on the inner face of plasma membrane, adding alternately glucuronic acid (GlcUA) and *N*-Acetylglucosamine (GlcNAc) to the reducing end of the growing chain (Weigel et al. 1997). The HAS enzyme alone is assumed to be responsible for the initiation and elongation of hyaluronan chains, and translocation of the growing chain through plasma membrane to extracellular space, presumably by forming a pore-like structure (Yoshida et al. 2000). It has been shown that GFP–XHAS1 is transported via the normal secretory pathway from ER and via Golgi to the plasma membrane (Mullegger et al. 2003), and HAS stays inactive until insertion to plasma membrane (Rilla et al. 2005). An inactive intracellular pool of HAS exists in the endoplasmic reticulum (ER), intracellular vesicles, and Golgi apparatus, perhaps as a reserve that may be rapidly transported to the plasma membrane in response to different stimuli (Rilla et al. 2005).

The three mammalian isoforms, HAS1, HAS2, and HAS3, are supposed to differ in their enzymatic properties (Itano et al. 1999a, b), overall activity (Brinck and Heldin 1999; Rilla et al. 2013), and in response to different stimuli (Jacobson et al. 2000). Has isoform mRNAs are differentially expressed in the developing embryo and in adult tissues (Spicer and McDonald 1998; Tien and Spicer 2005), and show also distinct expression patterns in different cell lines (Recklies et al. 2001; Yamada et al. 2004). Has2 knockout is lethal in mice, while Has1 and Has3 knockouts are viable with no obvious phenotypes (Camenisch et al. 2002). All isoforms of HAS are capable of pericellular hyaluronan coat formation (Brinck and Heldin 1999), but HAS1 forms a smaller coat as compared to HAS2 and HAS3 (Itano et al. 1999a, b; Rilla et al. 2013). HAS2 is the most active (Brinck and Heldin 1999) and most highly expressed isoform in many cells (Nishida et al. 1999). HAS3 has been found to synthesize shorter hyaluronan chains than other HASs when studied with membrane fragments in vitro (Brinck and Heldin 1999; Itano et al. 1999a, b; Spicer and Nguyen 1999), while cellular background seems to influence the molecular mass distribution (Brinck and Heldin 1999; Wilkinson et al. 2006).

The relatively low expression level of HASs in many cell types and lack of specific antibodies have impeded studies on their tissue distribution and subcellular localization, which has so far been possible only using fluorescent HAS fusion proteins (Kultti et al. 2006; Mullegger et al. 2003; Rilla et al. 2005; Spicer and Nguyen 1999). In the present work, we compared the immunohistochemical tissue distribution of the three HAS isoenzymes with the adjacent hyaluronan signal, and their subcellular localization with those of fluorescent HAS fusion proteins. The results of this work indicate that during embryonic development, the tissue distributions of HAS isoenzymes correspond well to those of previously reported mRNA levels. While the isoenzymes show individual spatial and temporal distributions in vivo, in most cases, the expressions are more or less overlapping. Their distribution at subcellular level is also partially overlapping, but the isoenzymes show distinct differences in their intracellular localization, probably reflecting different biological functions and suggesting differential regulatory mechanisms in their trafficking and activation.

Methods

Preparation of mouse embryo sections and stainings

C57Bl/6J mice were obtained from National Laboratory Animal Center, University of Kuopio, and housed there according to standard procedures. The Animal Care and Use Committee of the University of Kuopio approved the study protocols used in these experiments. For the fetal specimens, pregnant mice were killed 9, 11, 13, 15, and 17 d after copulation. The mouse embryos were fixed with 4 % paraformaldehyde in 0.1 M phosphate buffer (PB), pH 7.2. After overnight fixation, the specimens were washed in PB and dehydrated and embedded in paraffin. Sections of 5 μm thickness were cut and deparaffinized.

For HAS immunostainings, the sections were first incubated in 10 mM citrate buffer, pH 6.0 for 15 min at 120 °C in a pressure cooker. To block endogenous peroxidase, sections were treated for 5 min with 1 % H_2O_2, and after washes with PB, incubated in 1 % bovine serum albumin (BSA) and 0.1 % gelatine (Sigma G-2500, Sigma, MO) in PB for 30 min to block non-specific binding. The sections were incubated overnight at 4 °C with polyclonal antibodies for hyaluronan synthases HAS1 (2 μg/ml, sc-34021, Santa Cruz Biotechnology, inc., Santa Cruz, CA), HAS2 (2 μg/ml, sc-34067, Santa Cruz), or HAS3 (2 μg/ml sc-34204, Santa Cruz). After washes with PB, the sections were incubated for 1 h with biotinylated anti-goat antibody (1:1,000, Vector Laboratories) and with the avidin–biotin peroxidase method (1:200, Vectastain Kit, Vector Laboratories). The sections were incubated for 5 min in 0.05 % diaminobenzidine (Sigma, St. Louis, MO) and 0.03 % hydrogen peroxide in PB, yielding a brown reaction product. The specificities of the HAS antibodies were tested by incubating the antibodies with peptides used in the immunization.

For hyaluronan staining, sections were incubated with biotinylated complex of hyaluronan-binding region of bovine articular cartilage aggrecan G1 domain and link protein (bHABC) (Tammi et al. 1994) diluted in 1 % BSA, followed by avidin–biotin peroxidase and diaminobenzidine as described above. The specificity of the staining was controlled by blocking the bHABC probe with HA oligosaccharides. All sections were counterstained with Mayer's hematoxylin.

Stained sections were imaged with Zeiss Axio Imager. M2 light microscope (Carl Zeiss Microimaging GmbH, Zeiss, Jena, Germany).

Cell culture

The human breast adenocarcinoma cell line, MCF-7, was cultured in minimum essential medium alpha (MEMα, EuroClone, Pavia, Italy) supplemented with 5 % fetal bovine serum (FBS, HyClone, Thermo Scientific, Epsom, UK), 2 mM glutamine (EuroClone), 50 μg/ml streptomycin sulfate, and 50 U/ml penicillin (EuroClone). Cells were passaged twice a week at a 1:5 split ratio using 0.05 % trypsin (w/v) 0.02 % EDTA (w/v) (Biochrom AG, Berlin, Germany).

Human epidermal keratinocytes (HaCat cells) developed by Boukamp and co-workers (Boukamp et al. 1988)

were obtained from CLS (Heidelberg, Germany). HaCat and COS-1 cells were cultured in DMEM (High glucose, Gibco Paisley, Scotland, UK) supplemented with 10 % FBS (HyClone), 2 mM glutamine, 50 μg/ml streptomycin sulfate, and 50 U/ml penicillin (EuroClone).

Human dermal fibroblasts (from Dr. Michael Edward, University of Glasgow) were cultured in DMEM (Gibco) supplemented with 10 % FBS (HyClone), 2 mM glutamine, 50 μg/ml streptomycin sulfate, 50 U/ml penicillin (EuroClone), and 1 % nonessential amino acids (Gibco).

EGFP–hHas1, 2, and 3 fusion plasmid construction

The functional open reading frame (ORF) of human hyaluronan synthase 1 gene (Has1, NCBI Nucleotide accession number NM_001523), Has2 (NM_005328), and Has3 (NM_005329) ORFs were taken from human cDNA. The ORF of Has was amplified with a high-fidelity DNA polymerase (Phusion Hot start DNA polymerase, Finnzymes, Espoo, Finland). The primers for Has1 were 5′-ATA *CTC GAG* ag**A TG**A GAC AGC AGG ACG C (forward) and 5′-TAT *AAG CTT* c**TC AC**A CCT GGA CGC GGT A (reverse), containing the target sites for restriction endonucleases *Xho*I and *Hin*dIII (italics) and stuffers (minuscules) for in-frame ligation. The sites for translation initiation and termination are in boldface. The primers for Has2 were 5′-ACA*CTCGAG*at**A TG**C ATT GTG AGA GGT TTC (forward) and 5′-ACA *AAG CTT* c**TC AT**A CAT CAA GCA CCA TG (reverse), and for Has3 were 5′-GTA *CTC GAG* at**A TG**C CGG TGC AGC (forward) 5′-TAT *AAG CTT* c**TC AC**A CCT CAG CAA AAG CC (reverse) with the same restriction sites as above for Has1.

The sticky ends for the amplified Has ORFs as well as for the multiple cloning site of the vector pEGFP-C1 (Molecular Probes, Eugene, OR, USA) were produced with the above-mentioned restriction endonucleases (MBI Fermentas, Vilnius, Lithuania). Ligated (T4 DNA Ligase, Roche) DNA forming a fusion gene of EGFP and each of Has's were transfected into competent DH5α *E. coli* cells, which were prepared, propagated and purified. The integrity of the constructs was determined initially by restriction endonuclease digestion analysis and finally sequencing the junction sites and most of the ORF inserts.

Transfections

Subconfluent MCF-7 cell cultures were grown on 8-chamber slides (Ibidi GmbH, Martinsried, Germany) for microscopic inspection and on 24-well plates (CELL STAR®, Greiner Bio-One, Kremsmunster, Austria) for the measurements of hyaluronan in the culture media. Cells were transiently transfected with human Has cDNAs in-frame with an N-terminal GFP fusion protein (Molecular Probes, Eugene, OR, USA). The cells were examined next day after transfection.

Immunostainings of cultured cells

The cells grown on chambered cover glasses (Nalge Nunc, Naperwille, IL) coated with collagen type I (BD Biosciences, Bedford, MA) or 8-chamber slides (Ibidi GmbH, Martinsried, Germany) were fixed with 4 % paraformaldehyde in phosphate buffer, pH 7.4 (PB) for 1 h, washed with PB, permeabilized for 20 min at room temperature with 0.1 % Triton-X-100 in 1 % BSA, and incubated overnight at 4 °C with polyclonal antibodies for hyaluronan synthases HAS1 (2 μg/ml), HAS2 (2 μg/ml), or HAS3 (2 μg/ml), diluted in 1 % BSA alone, or combined with anti-Human Golgin-97 (1:100, Molecular Probes, Eugene, OR, USA) or Calnexin (1:100, Cell Signaling Technology, Inc., Boston, MA, USA) for double immunostainings. After washing, the cells were incubated for 1 h with Fluorescein or Texas red-labeled secondary antibodies (Vector Laboratories Inc., Burlingame, CA, l:1,000). To control cross-reactivity of the HAS antibodies, transiently transfected cells were immunostained with HAS antibodies utilizing avidin–biotin peroxidase method as described above. The human and mouse Has plasmids without fluorescent tag utilized in these control transfections were kindly provided by Dr. Paraskevi Heldin (Ludwig Institute for Cancer Research, Uppsala, Sweden).

Confocal microscopy

The fluorescent images were obtained with Zeiss LSM 700 confocal scanner on Zeiss Axio Observer inverted microscope and 63 × NA 1.4 oil-immersion objective (Carl Zeiss Microimaging GmbH, Zeiss, Jena, Germany) or with Ultraview® confocal scanner (PerkinElmer Life Sciences, Wallac-LSR, Oxford, UK), on a Nikon Eclipse TE300 microscope (Nikon, Tokyo, Japan) with a 60 × NA 1.4 oil-immersion objective. For the three-dimensional imaging, a series of horizontal optical sections were captured through the whole cell. The three-dimensional rendering of images and further modification was performed using ZEN 2009 software (Carl Zeiss Microimaging GmbH), ImageJ 1.32 software (http://rsb.info.nih.gov/ij/) and Adobe® Photoshop 8.0.

Assay of hyaluronan secretion

The culture media (containing serum) were collected for an enzyme-linked sorbent assays (ELSA) for hyaluronan, performed as described previously (Hiltunen et al. 2002; Rilla et al. 2005). Briefly, Maxisorp 96-well plates (Nunc)

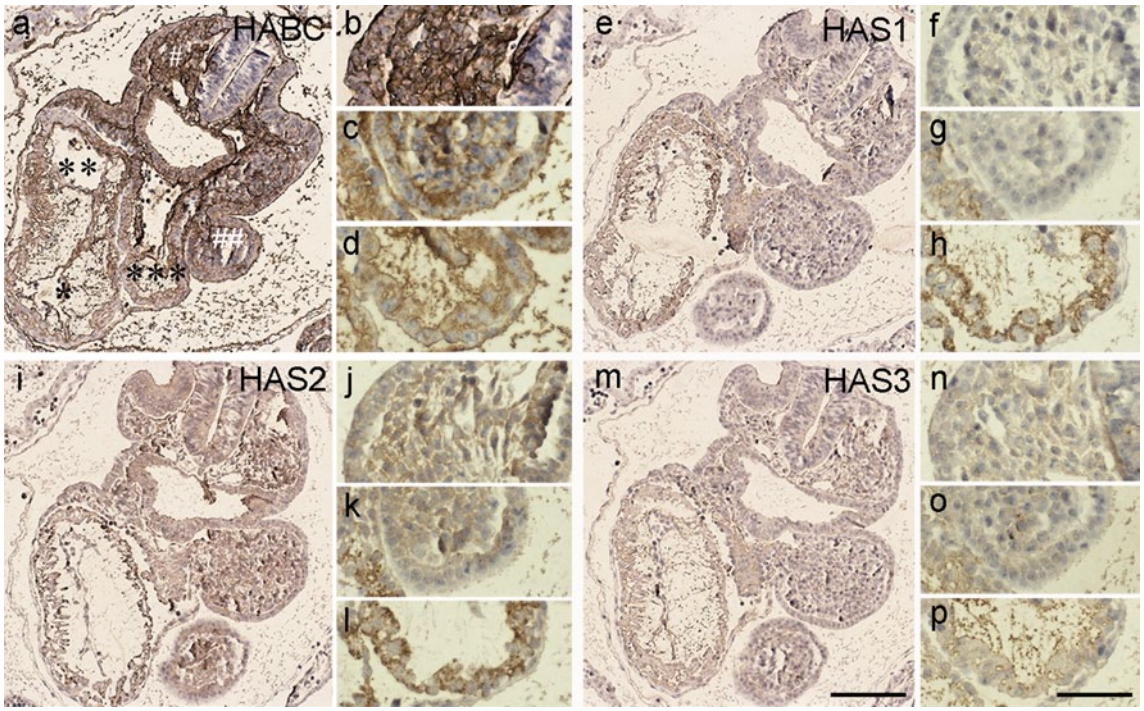

Fig. 1 Distribution of hyaluronan and hyaluronan synthases in E9 embryos. Mouse embryo sections (E9) were stained with bHABC to detect hyaluronan and HAS1, HAS2, HAS3 affinity-purified polyclonal antibodies to detect the HASs as described in "Materials and methods." *Brown color* indicates positive staining, and hematoxylin was utilized to stain nuclei (*blue*). *Panels* **a**, **e**, **i,** and **m** show whole embryos; **b**, **f**, **j,** and **n** mesenchyme around the neural tube in facial area; **c**, **g**, **k,** and **o** brachial arch; **d**, **h**, **l,** and **p** heart. *Asterisks* indicate the heart (*bulbus cordis, **aortic sac, ***common ventricular chamber), #indicates mesenchyme around the neural tube in facial area and ##in the brachial arch. *Magnification bars* 100 μm (**m**) and 50 μm (**p**)

were precoated with HABC (hyaluronan-binding complex, 1 μg/ml in 50 mM carbonate buffer, pH 9.5), washed with 0.5 % Tween-PBS, and blocked with 1 % BSA-PBS. The medium samples, diluted 1:40 or 1:50, and the hyaluronan standards (0–50 ng/ml, Provisc®, Algon, Fortworth, TX) were added into the wells and incubated for 1 h at 37 °C. The plates were then sequentially incubated with 100 μl of biotinylated HABC (1.0 μg/ml) and horse radish peroxidase streptavidin (1:20,000 in PBS, Vector), each for 1 h at 37 °C, and for 10 min at room temperature in the substrate–chromogen solution containing 0.01 % of 3,3′,5,5′-tetramethybenzidine and 0.005 % H_2O_2 in 0.1 M sodium acetate—1.5 mM citric acid buffer. The absorbances were measured at 450 nm after the addition of 50 μl of 2 M H_2SO_4.

Results

Hyaluronan and HAS stainings of paraffin-embedded tissue specimens

Mouse embryos from different developmental stages were collected, processed for histology, and stained with commercial anti-HAS antibodies and bHABC to detect HAS1-3 and hyaluronan (Figs. 1, 2, 3, 4). For comparison, human dermal specimens, rich in HA (Wang et al. 1992) and known to express all HAS isoforms (Mack et al. 2012; Yamada et al. 2004), were also stained for HAS (Fig. 5). The specificity of the hyaluronan stainings was controlled by preincubating bHABC with HA oligosaccharides (Tammi et al. 1994) and the HAS antibodies with the respective peptides used in the immunization. These control specimens showed reduced staining (Fig. 2). Additionally, the possible cross-reactivity between HAS antibodies was tested by overexpressing each HAS in MCF-7 breast cancer cell cultures and staining with HAS antibodies (Fig. 6). Deduced from the fact that an increased signal was detected only when staining with the corresponding antibody (Fig. 6), we assume that no cross-reactivity exists between the HAS isoform-specific antibodies.

E9 embryos

Strong hyaluronan staining was seen in the mesodermal layer around the neural tube and in the branchial arch (Fig. 1a–c). The different parts of the developing heart, bulbus cordis, aortic sac, and the common ventricular chamber

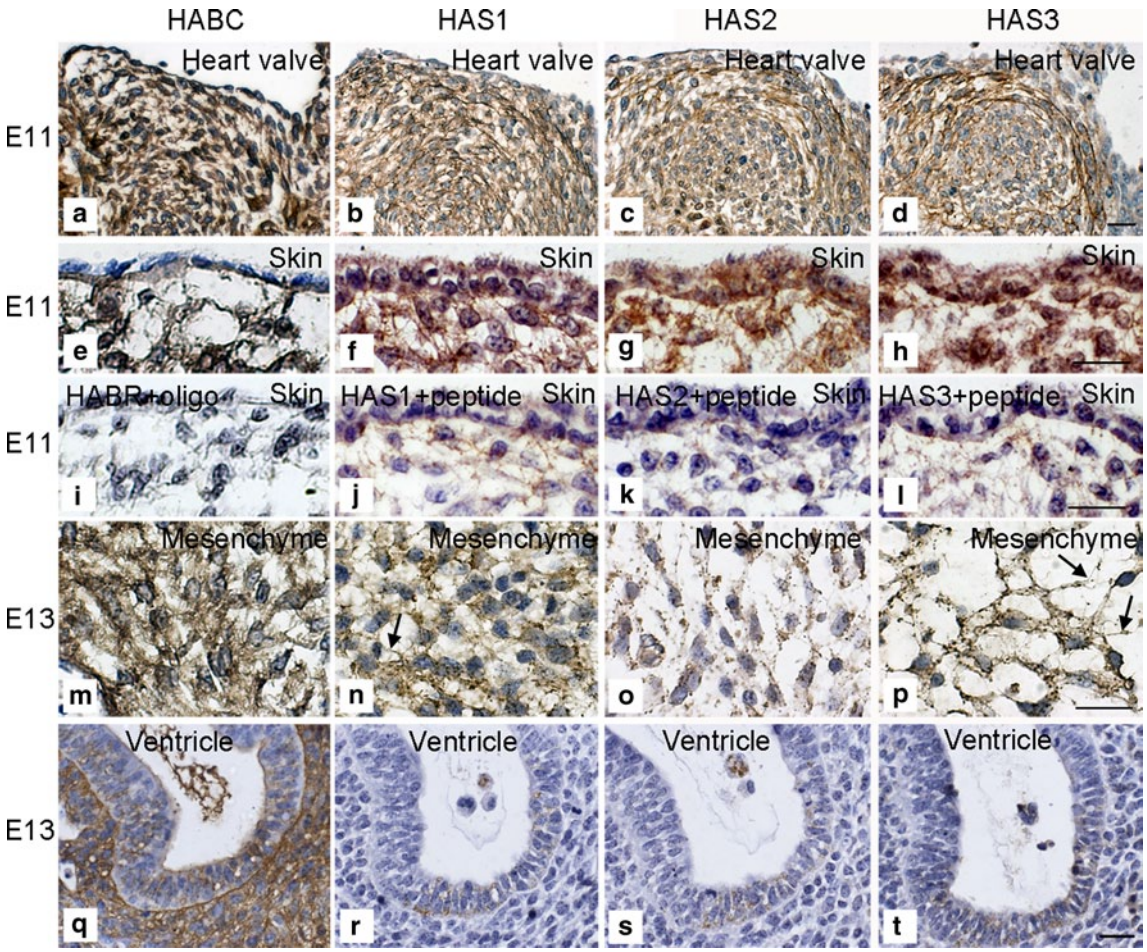

Fig. 2 Distribution of hyaluronan and hyaluronan synthases in E11–13 embryos. **a**-**l** E11, **m**-**t** E13. *Panels* **a**–**d**, developing heart valve; **e**–**l**, developing skin; **m**–**p**, mesenchyme from the area next to developing vertebral column; **q**–**t**, ventricle. In panel **i,** bHABC was pretreated with hyaluronan oligosaccharides prior to the staining and in **j**–**l,** the HAS antibodies were pretreated with respective peptides prior to the staining. *Arrows* in **n** and **p** indicate plasma membrane extensions. *Magnification bars* in all panels 20 μm

were also hyaluronan positive (Fig. 1a, d). While all HAS antibodies gave a positive staining at this stage, the staining intensity of HAS2 was highest and its tissue distribution largest (Fig. 1i–l). Thus, it stained all compartments of the heart and the mesodermal cells around the neural tube and in the branchial arch (Fig. 1i–l). HAS1 antibody stained the heart strongly (Fig. 1e, h), but the staining intensity of the mesodermal cells in the mesenchyme around the neural tube and the branchial arch was low (Fig. 1f, g). The distribution of HAS3 staining was similar to HAS1 but of lower intensity (Fig. 1m–p).

E11–13 embryos

At these developmental stages, the heart was very intensely stained with bHABC and all HAS antibodies, both in the valve area (Fig. 2a–d) and elsewhere in the heart wall (data not shown). The HAS1–3 antibodies showed similar staining intensities in the heart. Very intense HA and HAS stainings were also detected in the mesenchymal tissues like skin dermis (Fig. 2e–h) and at the sites of the future skull bones of mesenchymal origin (Fig. 2m–p). In the latter location, the staining intensities of HAS3 and HAS1 were higher than that of HAS2 (Fig. 2m–p). Although most epithelial tissues were hyaluronan and HAS negative at this stage, the epithelium in the ventricle showed a faint staining for them (Fig. 2q–t).

E15 embryos

The mesenchymal tissues all through the body were intensely hyaluronan positive at this stage (Fig. 3a), as also seen in the higher power images from oral mucosa (Fig. 3b), skin (Fig. 3c), and the wall of thorax (Fig. 3m). At these sites, all HAS antibodies stained the mesenchymal cells, but the staining intensity for HAS2 was highest

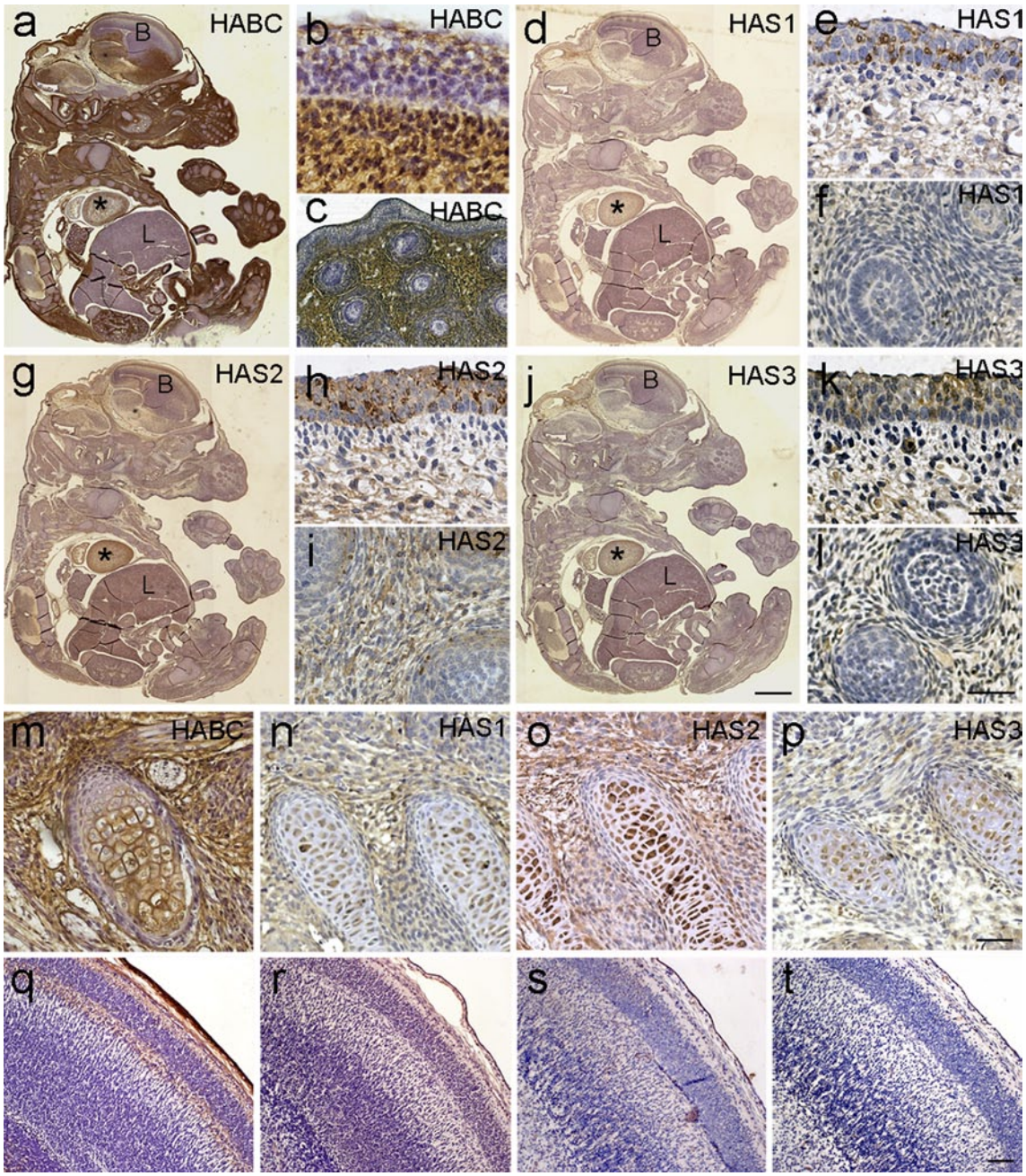

Fig. 3 Distribution of hyaluronan and hyaluronan synthases in E15 embryos. Mouse embryonic tissues were stained for HA and HAS1–3. *Panels* **a**, **d**, **g,** and **j** show sagittal sections of whole embryos. *Panels* **b**, **e**, **h,** and **k** show oral mucosa; **c**, **f**, **i,** and **l**, skin in the snout containing vibrissa follicles; **m**–**p** cartilages in the vertebral column, and **q**–**t** cortex of the brain. *B* brain, *L* liver, *heart. *Magnification bars* 1 mm (**j**) and 50 μm (**k**, **l**, **p**, **t**)

(Fig. 3e–l, n–p). Cartilages were intensely stained with bHABC, the cells within cartilage showing more intense staining than those in the surface (Fig. 3m). Similarly, HAS1–3 antibodies intensely stained the chondrocytes in the interior of the cartilages (Fig. 3n–p). In E15 embryos, heart was positive for HA and all HASs, while liver and the major parts of the central nervous system were negative (Fig. 3a, d, g, j). At this stage, the stratified epithelia in the mouth and skin started to express hyaluronan (Fig. 3b and data not shown), and they were also positive for all HASs (Fig. 3e, h, k and data not shown). The hyaluronan and HAS stainings in the vibrissae follicles, which are derived from the surface epithelium, were faint, but at least HAS2 could be detected (Fig. 3i).

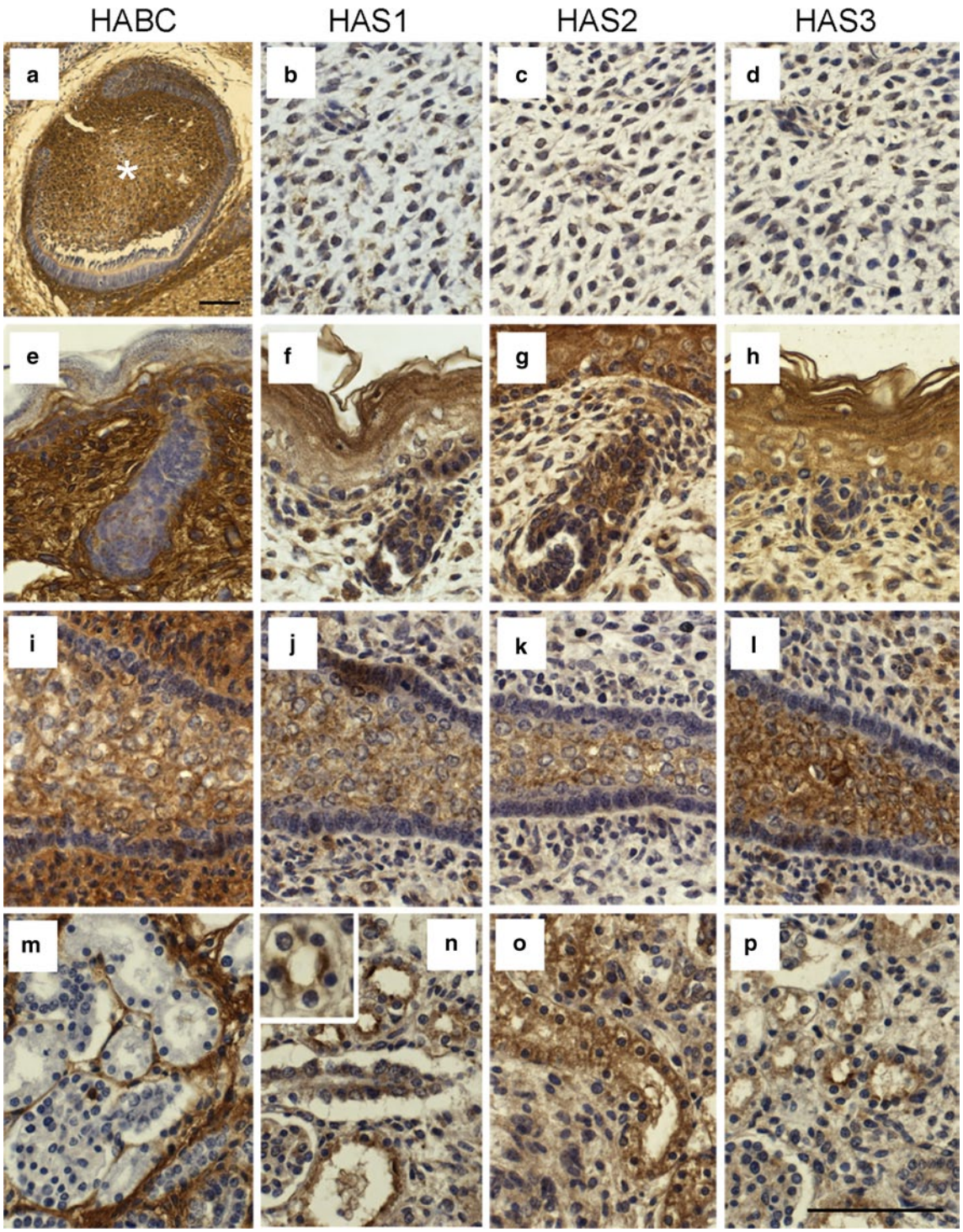

Fig. 4 Distribution of hyaluronan and hyaluronan synthases in E15 embryos. *Panels* **a**–**d** show vitreous (*asterisks* in **a**) in developing eye; **e**–**h**, developing skin and hair follicles; **i**–**l**, the web between the fingers of the hand; **m**–**p**, developing kidney. *Magnification bars* in all panels 50 μm

E17 embryos

Mesenchymal tissues continued to express high amounts of hyaluronan and HASs as indicated by the stainings of the skin (Fig. 4). Although most cartilages appeared negative for hyaluronan at this stage, they continued to show a signal for all HAS isoforms (data not shown). The negative hyaluronan staining is probably due to the masking caused by large proteoglycans (Parkkinen et al. 1996). At the start of ossification, the newly formed

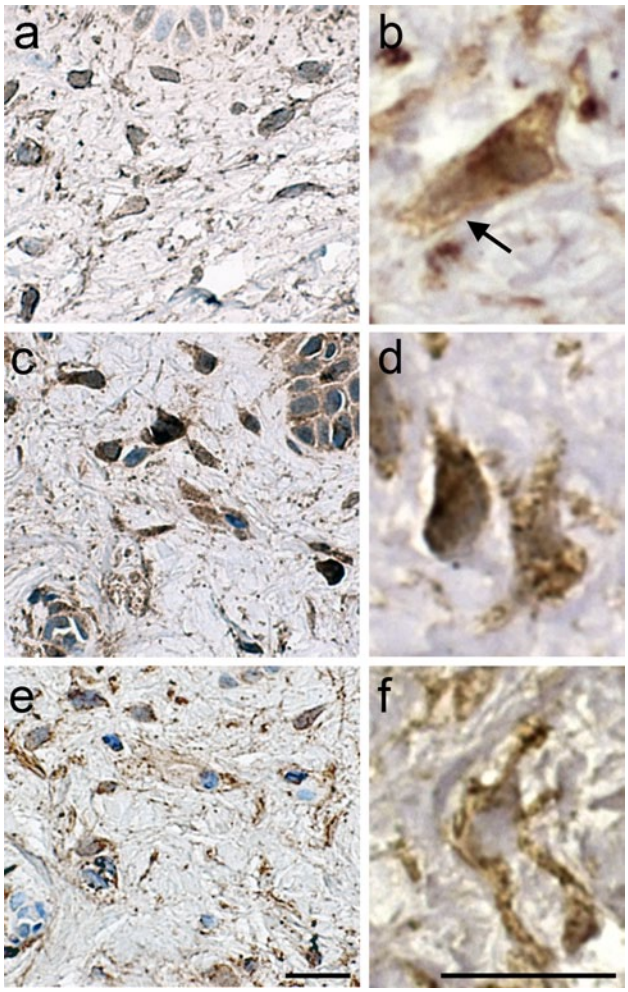

Fig. 5 All HAS isoforms show positive staining in human skin dermal fibroblasts. Staining of HAS1 (**a**, **b**), HAS2 (**c**, **d**), and HAS3 (**e**, **f**) in human skin sections. Overall, dermal staining is shown in **a**, **c,** and **e**. A higher magnification of dermal fibroblasts is shown in **b**, **d,** and **f**. *Arrow* in **b** indicates plasma membrane staining. *Magnification bars* 20 μm

osteocytes were positive for HAS2 and HAS3 (data not shown).

The vitreous body was intensely stained with bHABC, but the staining intensities for HASs were low (Fig. 4a–d). The epidermis, fully mature at this stage, showed intense staining for hyaluronan and HAS2 and HAS3, while HAS1 staining was of lower intensity (Fig. 4e–h). Similar strong hyaluronan and HAS stainings were observed in stratified epithelia in other locations, like mouth and esophagus (data not shown). In the uppermost layers of stratified epithelia, all HAS antibodies gave a strong signal, which may be partly due to unspecific staining of stratum corneum (Fig. 4f–h); especially, strong hyaluronan and HAS stainings were detected in the paw epidermal areas of the future cleft between the fingers (Fig. 4i–l), and also between the lip and the gum (data not shown), and between eye lids (data not shown). While the growing hair follicles showed just faint positivity for hyaluronan, similar to the vibrissae follicles, there was a distinct signal for HASs in the follicles (Fig. 4e–h). In the developing kidneys, the stromal connective tissue was intensely hyaluronan positive while most of the tubules were negative for hyaluronan (Fig. 4m–p). All HAS antibodies stained the kidneys. Interestingly, the HAS staining was mainly localized in the tubular cells, while the stromal cells were negative (Fig. 4n–p). The HAS1 and HAS3 stainings were limited just to a part of the tubular structures, while HAS2 distribution was more widespread, staining for example most of the collecting tubules (Fig. 4n–p).

Subcellular localization of HAS in developing mouse tissues

The main subcellular location with all HAS antibodies was the cytoplasm (Figs. 1, 2, 3, 4). However, occasional plasma membrane localization was seen, for example, in developing heart (Fig. 1), and in the epidermal cells of the webs between fingers (Fig. 4i–l). HAS2 immunostaining in the tubules of the kidney was either intracellular or on the plasma membrane, without clear preference (Fig. 4o), while HAS1 and HAS3 showed occasionally a strong apical signal (Fig. 4n, insert and p). The mesenchymal cells of the future intramembranous bones formed long plasma membrane extensions, which were intensely stained, especially with HAS1 and HAS3 antibodies (Fig. 2n, p, arrows).

Correlation of HAS immunostainings with hyaluronan

Staining of one or several HASs was usually associated with hyaluronan accumulation in the tissues. For example, at E9, hyaluronan staining correlated with HAS2 staining, while at E11, heart valves were intensely positive for hyaluronan and all HAS isoforms. Mesenchymal cells in the developing skin were also rich in HA, and the expression of all HAS isoenzymes was detected. In contrast, the cortex of the brain was negative for all HAS isoforms (Fig. 3r, s, t) and did not contain any hyaluronan, either (Fig. 3q). In the oral epithelium and in the web of the limbs, the appearance of hyaluronan staining temporarily coincided with HAS immunostainings (Figs. 3, 4). There were some exceptions in the positive correlation between hyaluronan and HASs. Thus, vitreous body was intensely stained with bHABC in E17 specimens (Fig. 4a), while HAS staining intensities were almost absent, (Fig. 4b–d). The same was seen in the mesenchyme around the ventriculus. Furthermore, in kidneys, the tubules were hyaluronan negative, but expressed all HAS isoforms (Fig. 4). Instead, the stromal tissue between the tubules was strongly HA positive, but was just faintly positive for HAS2 and HAS3. In this case,

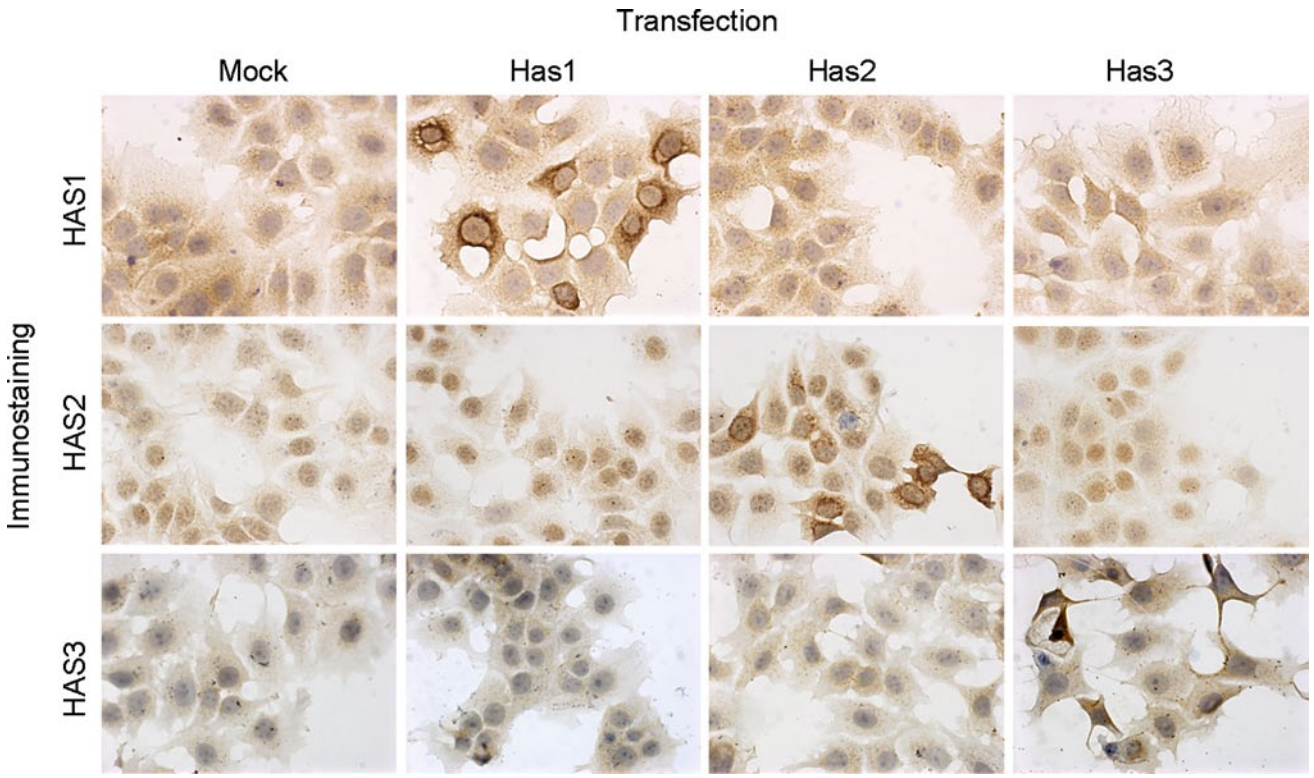

Fig. 6 The specificity and possible cross-reactivity between HAS antibodies was tested by overexpressing each HAS in MCF-7 breast cancer cell cultures by transient transfection. The MCF-7 cells have normally very low endogenous levels for HASs. The fixed cell cultures were stained with each HAS antibody (Has1 overexpressing cells were stained with HAS1, HAS2, and HAS3 antibodies; Has2 overexpressing cells were stained with HAS1, HAS2, and HAS3 antibodies. *Brown color* indicates positive staining, and hematoxylin was utilized to stain nuclei (*blue*)

the apparent discrepancy may be explained by the diffusion of hyaluronan from the site of synthesis in the tubules to the stroma.

In general, HAS2 was most abundant, both in tissue distribution and staining intensity, and HAS3 antibody gave the weakest signal in mouse embryonic tissues, in line with the findings on their mRNA levels during embryonic development (Tien and Spicer 2005).

HAS immunostaining of dermal cells in human skin

The antibodies used in the present study were generated against peptides, which are identical in mouse and human HASs. To confirm that they also work in human tissues, we stained adult human skin, where fibroblasts are known to express all HAS isoforms (Mack et al. 2012; Yamada et al. 2004), with the anti-HAS antibodies. Strong HAS1, HAS2, and HAS3 signals were detected in dermal fibroblasts (Fig. 5), in agreement with the high intensity of immunostainings in fibroblast cell cultures (Fig. 7a–c). Plasma membrane staining was sometimes seen, as indicated by the high power image of HAS1 (Fig. 5b, arrow), while a large proportion of HAS was observed in intracellular vesicles (Fig. 5b, d, f). These findings were also in line with the staining pattern of mouse embryonic tissues (Figs. 1, 2, 3, 4) and cell cultures (Fig. 7).

Localization of HASs in cultured cells

Immunostainings of endogenous HASs

To study the subcellular localization of different HASs in more detail, we used three different cell types with different Has mRNA expression and hyaluronan secretion levels (Table 1), and the same antibodies as in the staining of tissues sections (Figs. 7, 8). Human skin dermal fibroblasts which express high levels of Has 1, 2, and 3 isoforms (Jokela, unpublished) and secrete high levels of hyaluronan (Table 1) were intensely stained with all HAS antibodies (Fig. 7a–c). The human keratinocyte cell line, HaCat, which also expresses all Has isoforms but secretes less hyaluronan than fibroblasts, was stained with anti-HAS2 and anti-HAS3 antibodies, while the signal with anti-HAS1 antibody was low (Fig. 7d– f). COS-1 cells were negative when stained with the HAS antibodies, except the occasional, small HAS-positive vesicles (Fig. 7g–i), in line with

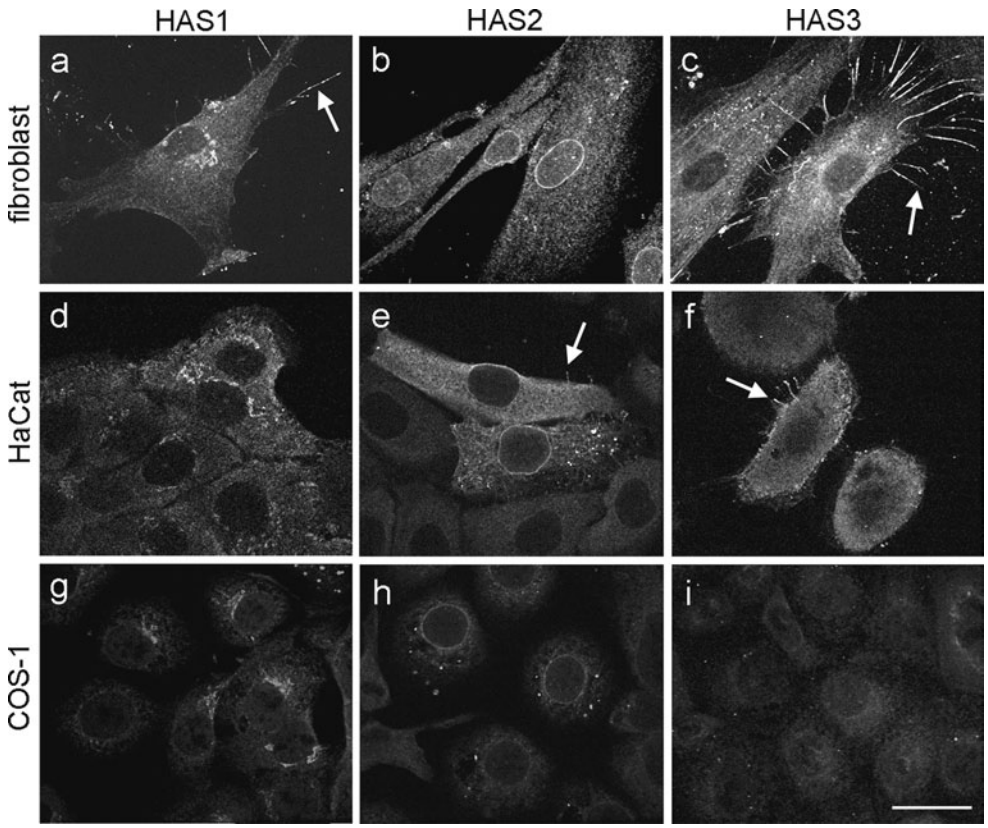

Fig. 7 Staining intensity and localization of the endogenous HASs differs in different cell lines. Cultured cells in subconfluent monolayer cultures were immunostained with antibodies against HAS1 (**a**, **d**, **g**), HAS2 (**b**, **e**, **h**), and HAS3 (**c**, **f**, **i**). Compressed image stacks of confocal optical sections are shown in **a**–**c** and optical sections in **d**–**i**. Human dermal fibroblasts are shown in (**a**–**c**), human epidermal keratinocytes, HaCat in (**d**–**f**) and COS-cells in (**g**–**i**). Magnification bar 20 μm

Table 1 Endogenous hyaluronan secretion into the culture media of different cell types

Cell type	Hyaluronan production ng/10,000 cells/24 h
Human skin fibroblasts	22.6 ± 2.83
Human keratinocytes (HaCat)	10.0 ± 0.68
COS-1 cells	0.50 ± 0.21

Mean ± SD of 3 wells

the low mRNA levels for all HAS isoforms (Jokela, unpublished) and negligible amounts of hyaluronan secreted by these cells (Table 1).

All HAS isoforms were detected both in intracellular locations and on plasma membrane. However, there were differences in the relative distribution between the isoforms. Thus, HAS3 accumulated in plasma membrane and its protrusions, with a relatively smaller intracellular pool as compared to other HASs (Fig. 7c, f). HAS1 staining was mainly localized intracellularly, although it was also detectable in plasma membrane and its protrusions (Fig. 7a, d), whereas most of the HAS2 staining was localized in cytoplasmic vesicles with occasional localization on the plasma membrane (Fig. 6b, e). The dual staining of fibroblasts with HAS1 antibody and Golgi marker showed that most of the intracellular HAS1 was localized in Golgi area (Fig. 8a–c). The dual staining of HaCat with HAS2 antibody and the ER-marker calnexin showed that most of the intracellular HAS2 was localized in ER, with a special accumulation in perinuclear area, probably in nuclear membrane (Fig. 8d–f). The perinuclear staining with HAS2 antibody was especially prominent in fibroblasts (Fig. 7b), in primary mouse keratinocytes, and in rat keratinocytes (data not shown). Dual staining with bHABC showed HAS3 association with plasma membrane ruffles (Fig. 8g–i) and long protrusions (Figs. 7, 8j–l), both structures with strong surface hyaluronan positivity (Fig. 8i, l, arrows).

Localization of human GFP–HAS1–3 expressed in MCF-7 cells

To support the findings about the differential subcellular localization of HAS isoforms, we compared the subcellular

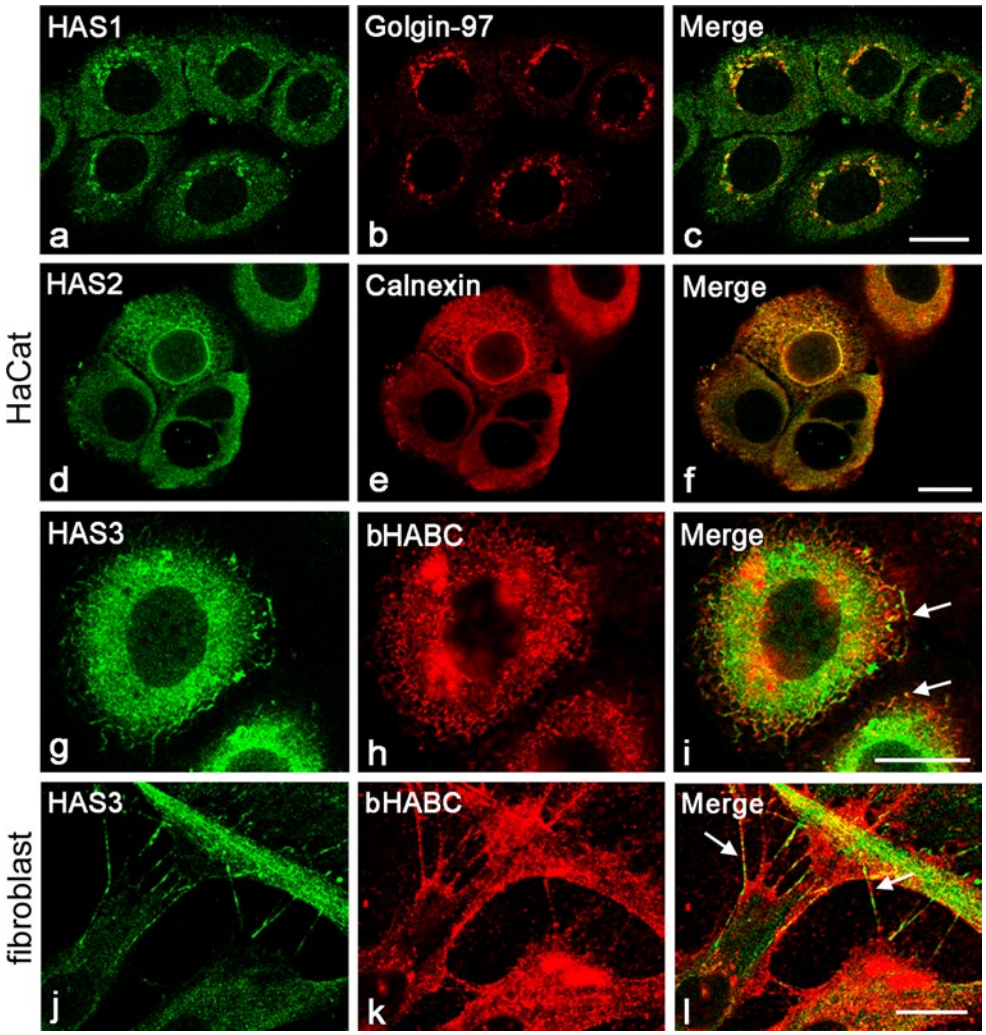

Fig. 8 Endogenous HASs differ in their distribution in subcellular compartments. HaCat cells (**a**–**c**) stained with HAS1 antibody (*green*) (**a**) and Golgi marker (*red*) (**b**) and merged image (**c**). HaCat cells stained for HAS2 antibody (*green*, **d**), ER marker (calnexin, *red*, **e**) and a merged image (**f**). HaCat cells (**g**–**i**) and fibroblasts (**j**–**l**) stained with HAS3 antibody (*green*, **g**, **j**) and bHABR (*red*, **h**, **k**) and merged images (**i**, **l**). *Magnification bars* 20 μm

distribution of recombinant HASs with fluorescent protein tags. For that purpose, we transiently transfected MCF-7 cells, which endogenously secrete low amounts of hyaluronan, with human GFP–HAS constructs. Each HAS isoform had a typical subcellular distribution (Fig. 9). GFP–HAS1 was accumulated in intracellular compartment, including a net-like pattern (ER) and accumulation in Golgi area (Fig. 9a). GFP–HAS1 was also localized in vesicles near the plasma membrane and on thin plasma membrane protrusions (arrow in Fig. 9a). GFP–HAS2 was also mainly accumulated in intracellular vesicles, representing ER, Golgi, and transport vesicles (Fig. 9c, d). On the plasma membrane, GFP–HAS2 was localized on irregularly spaced protrusions, especially located in the edges of lamellipodia (arrow in Fig. 9d). GFP–HAS3 had an intracellular pool too, but it was very clearly accumulated on numerous, regularly spaced plasma membrane protrusions covering the whole apical cell surface (Fig. 9e, arrow in f). It is obvious that the Golgi area was overemphasized in the GFP–HAS-expressing cells, but the overall distribution of GFP–HASs corresponded to that seen in immunostainings.

Discussion

The levels and localizations of HAS isoforms are likely to be highly important in processes like embryonic development, wound healing, inflammation, and malignant growth, but have been difficult to study due to the lack of reliable antibodies. In the present work, we characterized commercial antibodies against different HAS isoforms by comparing the immunostaining results with published mRNA

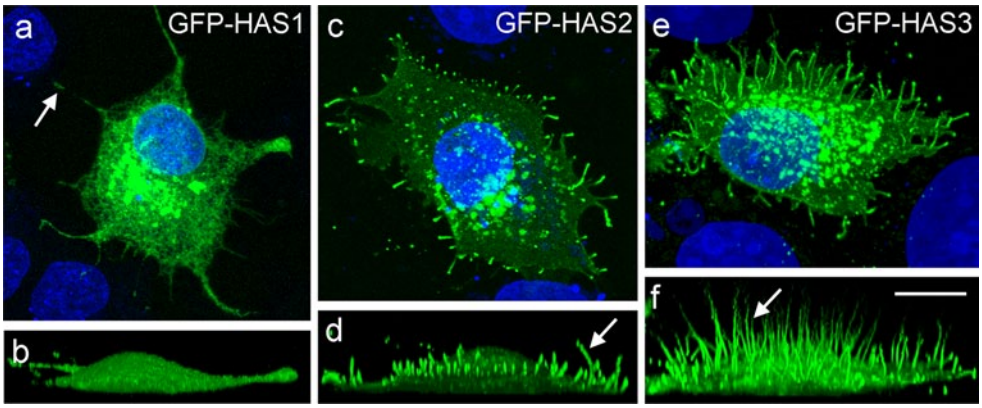

Fig. 9 Each recombinant EGFP–HAS isoform has a typical subcellular distribution in MCF7 cells. Localization of HAS1 (**a**, **b**), HAS2 (**c**, **d**), and HAS3 (**e**, **f**), transfected as fluorescent EGFP fusion proteins in MCF-7 cells. The panels (**a**, **c**, **e**) show compressed stacks of horizontal optical sections and vertical views obtained from primary image stacks (**b**, **d**, **f**). *Arrows* indicate HAS-positive protrusions. *Magnification bar* 10 μm

expression levels in tissues and cells, and by comparing the subcellular localization of endogenous, immunostained HASs with those obtained with the expression of GFP-labeled recombinant proteins. In general, the antibodies proved to give results that were in accordance with mRNA levels and hyaluronan synthesis. The peptide controls and cross-staining experiments following transfections with different HASs indicated that the stainings were specific and that there was no cross-reactivity between the HAS isoforms.

Distribution of HAS isoenzymes in embryonic mouse tissues

The tissue distributions of different HAS isoforms corresponded well with the reported mRNA expression levels in different organs during the embryonic development (Tien and Spicer 2005). For example, heart valves at E9 and 11 reported to express high levels of HAS2 and were also intensely positive in HAS2 immunostainings, while tissues exhibiting low Has2 mRNA expression levels like brain showed low immunostaining with HAS antibodies. The same correlation was also found in cultured cell lines. Skin fibroblasts expressing high levels of all HAS isoforms (Rilla et al. 2013) were strongly immunostained with all HAS antibodies, while COS-1 cells with low levels of Has mRNAs (Rilla et al. 2013) were also negative in immunostaining. Although the HAS isoforms showed overlapping distribution in the immunostainings of many tissues and cells, this was not due to the cross-reactivity between the HAS isoforms as cells lacking a certain HAS mRNA were also negative in the corresponding immunostainings. However, although the HAS immunostainings were often in line with the reported mRNA levels (Tien and Spicer 2005), the correlation was not observed in some regions, like vibrissa follicles (Tien and Spicer 2005). Similarly, the mRNA and protein levels did not correlate in ovarian and endometrial tissues (Nykopp et al. 2009, 2010). Differences in HAS protein turnover rate may explain the discrepancy (Tammi et al. 2011; Vigetti et al. 2012).

A high level of HAS protein immunoreactivity correlated with strong hyaluronan staining in many tissues like cartilage and developing heart. On the other hand, in vitreous body and the stromal compartment of developing kidney, the HAS immunostainings were of low intensity despite the very intense hyaluronan staining. The turnover of hyaluronan itself varies in different tissues and is reported to be very slow in the adult vitreous body (Laurent and Fraser 1986). Posttranslational modifications of HAS enzymes or the precursor sugar supply are important regulators of HAS activity (Tammi et al. 2011) and show differences between different tissues and cell types (Rilla et al. 2013). Hyaluronan may also diffuse to the target tissue from the neighboring cells with high hyaluronan-synthesizing activity. The HAS isoenzymes also differ in their requirement for the substrate levels, HAS1 being practically inactive at UDP sugar levels present in many cell types (Rilla et al. 2013). This may at least partially explain why HAS1, although present in E9 embryonic heart, cannot compensate for the loss of HAS2 (Camenisch et al. 2000). On the other hand, the overlapping expression of HAS isoenzymes in many tissues of mesodermal origin, like developing cartilages, may explain why HAS1 KO, HAS3 KO, and HAS1/HAS3 double KO mice do not create skeletal malformations despite their relatively strong expressions in these tissues. Whether HAS3 or HAS1 could compensate the loss of HAS2 in these tissues is at the moment unknown as HAS2 KO mice die early, before the development of skeleton. Tissue-specific or inducible KO of HAS2 will help to resolve this question and to find whether HAS2

plays a role in the development of other organs like the kidney where it appears to be the main isoform in a part of the developing tubules.

Subcellular distribution of HAS isoenzymes

Immunostaining of all HAS isoenzymes was found in intracellular locations and on the plasma membrane, both in cultured cells and tissue sections. The survey of the embryonic samples suggested that there are also tissue-specific differences in the localization of each HAS, like the preferential apical localization of HAS1 and 3 in kidney tubules, perhaps indicating cell-specific regulation of the localization of HAS/HA synthesis. The immunostainings support our conclusions based on the GFP-tagged HASs on the HAS transport pathway from ER via Golgi to plasma membrane, and possible recycling or degradation in lysosomes (Rilla et al. 2005), although the artificial overexpression seems to slightly exaggerate their accumulation in Golgi and ER. This was evident for HAS3, which showed relatively lower immunostaining in Golgi as compared to the signal from GFP.

The differences in the relative proportion of intracellular versus plasma membrane-associated HAS raise several questions. The low signal of HAS2 on the plasma membrane may be due to masking of the antigen site of the antibody. However, GFP–HAS2 shows a similar distribution, supporting the conclusion that HAS2 may form a large intracellular pool. HAS2 and HAS3 have to be inserted to the plasma membrane to be synthetically active (Rilla et al. 2005), while HAS1 has been suggested to be able to synthesize hyaluronan also in intracellular locations (Ghosh et al. 2009). The lower proportion of HAS2 on plasma membrane compared to HAS3, a difference which is also evident with immunostainings of the proteins, may reflect differential turnover time or stability of HAS2 and HAS3 on the plasma membrane. Itano and co-workers reported that in plasma membrane preparations, HAS3 retained its activity at least for 8 h, while HAS2 lost it in 3 h and HAS1 already in 1 h (Itano et al. 1999a, b). The turnover time of the HAS protein may differ under different conditions in live cells, too (Bansal and Mason 1986; Kitchen and Cysyk 1995), suggesting that the differences in the lifetime between the HAS proteins may explain the different subcellular localizations of the HASs.

Endogenous HAS2 is accumulated in ER/Golgi, forming a large pool of an inactive form, which could be rapidly mobilized and transported to the plasma membrane for activation. The transport of endogenous HAS3, showing less accumulation inside the cells, could be constitutive rather than regulated. This fits with the hypothesis that HAS3 functions under basal conditions and HAS2 are more dynamic in its response to various stimuli (Jacobson et al. 2000; Suzuki et al. 2003). Activation of the existing protein stores would give an instant response in conditions like wounding (Maytin et al. 2004; Tammi et al. 2005), irritation, or inflammation (Mack et al. 2012), whereas the transcriptional regulation, although important in HAS2 regulation (Karvinen et al. 2003; Pasonen-Seppänen et al. 2003; Pienimäki et al. 2001), requires several hours. HAS2 contains putative phosphorylation sites for PKC- and cAMP-dependent kinases (Vigetti et al. 2011; Ohno et al. 2001), as well as sites for O-GlcNAcylation (Vigetti et al. 2012), suggesting that its activity could be regulated by these modifications. However, as HAS3 is also be phosphorylated (Goentzel et al. 2006), its activity may also experience some posttranslational control.

HASs in plasma membrane extensions

Human EGFP–HAS3 and EGFP–HAS2 constructs transfected in MCF-7 cells induced similar long plasma membrane extensions as the mouse HAS3 and HAS2 constructs (Kultti et al. 2006). The HAS isoenzymes differ in their ability to induce the extensions, HAS3 being the most effective, while HAS1 overexpression induced practically no extensions. Immunostainings with antibodies against HAS isoenzymes showed similar staining in membrane extensions, even in tissues in vivo. Despite the inability of HAS1 overexpression to induce extensions, GFP–HAS1 was localized in the natural extensions when they are present. The formation of extensions requires active hyaluronan synthesis, but the differences in the ability to form them are not only explained by differences in the rate of hyaluronan synthesis, as both HAS2 and HAS3 overexpressions induced high hyaluronan production. The extensions induced by HAS are dependent on actin cytoskeleton, and it is possible that there are special cytoskeletal foci (Weinbaum et al. 2007) or membrane specializations like lipid rafts (Kultti et al. 2006) that determine the formation of the extensions, and that the ability to interact with them differs between HAS isoenzymes.

Conclusions

The present study shows that the three HAS isoenzymes show overlapping expression in many tissues, especially in mesenchymal cells. There are also temporal differences in their expression, so that HAS2 appears to be the main isoform during early embryogenesis, as also indicated by the lethality of its knockout at this stage. In the kidneys, part of tubules appears to express mainly HAS2. The expression of isoenzymes is known to be differentially regulated by growth factors, cytokines, and hormones (Jacobson et al. 2000), and the present data suggest that there are also

differences in their subcellular localization that probably correlates with their activity. As most cell types express more than one HAS, and the isoenzymes may form heterodimers (Karousou et al. 2010), the temporally and spatially overlapping expressions of the different HAS isoforms may create a new control system for hyaluronan synthesis. Because of the overlapping expressions of HAS isoenzymes in several tissues, tissue-specific KO of each HAS isoenzyme or the induction of the deletion at a certain time point is needed to get a more complete view about their significance during the development. Furthermore, as hyaluronan synthesis plays a role in stress reactions and inflammation, it is important to use isoenzyme-specific knockdown of HAS to reveal their roles in these conditions.

Acknowledgments Special thanks are due to Eija Kettunen, Kari Kotikumpu, Eija Rahunen, and Arja Venäläinen for expert technical assistance. This work was supported by the Academy of Finland, Grant #40807 and #54062 (M.T.), and by the grants from The North Savo Cultural Foundation (K.R.), Kuopio University Foundation (K.R.), The North Savo Cancer Foundation (K.R), Paavo Koistinen Foundation (K.R. and K.T.), The Finnish Cancer Foundation (R.T.), Sigrid Juselius Foundation (RT and MT), The Spearhead Funds of the University of Eastern Finland (Cancer Center of Eastern Finland), and the EVO funds of Kuopio University Hospital (M.T.).

References

Bansal MK, Mason RM (1986) Evidence for rapid metabolic turnover of hyaluronate synthetase in Swarm rat chondrosarcoma chondrocytes. Biochem J 236:515–519

Boukamp P, Petrussevska RT, Breitkreutz D, Hornung J, Markham A, Fusenig NE (1988) Normal keratinization in a spontaneously immortalized aneuploid human keratinocyte cell line. J Cell Biol 106:761–771

Brinck J, Heldin P (1999) Expression of recombinant hyaluronan synthase (HAS) isoforms in CHO cells reduces cell migration and cell surface CD44. Exp Cell Res 252:342–351

Camenisch TD, Spicer AP, Brehm-Gibson T, Biesterfeldt J, Augustine ML, Calabro A Jr, Kubalak S, Klewer SE, McDonald JA (2000) Disruption of hyaluronan synthase-2 abrogates normal cardiac morphogenesis and hyaluronan-mediated transformation of epithelium to mesenchyme. J Clin Invest 106:349–360

Camenisch TD, Schroeder JA, Bradley J, Klewer SE, McDonald JA (2002) Heart-valve mesenchyme formation is dependent on hyaluronan-augmented activation of ErbB2-ErbB3 receptors. Nat Med 8:850–855

Ghosh A, Kuppusamy H, Pilarski LM (2009) Aberrant splice variants of HAS1 (Hyaluronan Synthase 1) multimerize with and modulate normally spliced HAS1 protein: a potential mechanism promoting human cancer. J Biol Chem 284:18840–18850

Goentzel BJ, Weigel PH, Steinberg RA (2006) Recombinant human hyaluronan synthase 3 is phosphorylated in mammalian cells. Biochem J 396:347–354

Hiltunen EL, Anttila M, Kultti A, Ropponen K, Penttinen J, Yliskoski M, Kuronen AT, Juhola M, Tammi R, Tammi M, Kosma VM (2002) Elevated hyaluronan concentration without hyaluronidase activation in malignant epithelial ovarian tumors. Cancer Res 62:6410–6413

Itano N, Sawai T, Miyaishi O, Kimata K (1999a) Relationship between hyaluronan production and metastatic potential of mouse mammary carcinoma cells. Cancer Res 59:2499–2504

Itano N, Sawai T, Yoshida M, Lenas P, Yamada Y, Imagawa M, Shinomura T, Hamaguchi M, Yoshida Y, Ohnuki Y, Miyauchi S, Spicer AP, McDonald JA, Kimata K (1999b) Three isoforms of mammalian hyaluronan synthases have distinct enzymatic properties. J Biol Chem 274:25085–25092

Jacobson A, Brinck J, Briskin MJ, Spicer AP, Heldin P (2000) Expression of human hyaluronan synthases in response to external stimuli. Biochem J 348(Pt 1):29–35

Karousou E, Kamiryo M, Skandalis SS, Ruusala A, Asteriou T, Passi A, Yamashita H, Hellman U, Heldin CH, Heldin P (2010) The activity of hyaluronan synthase 2 is regulated by dimerization and ubiquitination. J Biol Chem 285:23647–23654

Karvinen S, Pasonen-Seppänen S, Hyttinen JM, Pienimäki JP, Törrönen K, Jokela TA, Tammi MI, Tammi R (2003) Keratinocyte growth factor stimulates migration and hyaluronan synthesis in the epidermis by activation of keratinocyte hyaluronan synthases 2 and 3. J Biol Chem 278:49495–49504

Kitchen JR, Cysyk RL (1995) Synthesis and release of hyaluronic acid by Swiss 3T3 fibroblasts. Biochem J 309(Pt 2):649–656

Kultti A, Rilla K, Tiihonen R, Spicer AP, Tammi RH, Tammi MI (2006) Hyaluronan synthesis induces microvillus-like cell surface protrusions. J Biol Chem 281:15821–15828

Laurent TC, Fraser JR (1986) The properties and turnover of hyaluronan. Ciba Found Symp 12487132709:9–29

Mack JA, Feldman RJ, Itano N, Kimata K, Lauer M, Hascall VC, Maytin EV (2012) Enhanced inflammation and accelerated wound closure following tetraphorbol ester application or full-thickness wounding in mice lacking hyaluronan synthases Has1 and Has3. J Invest Dermatol 132:198–207

Maytin EV, Chung HH, Seetharaman VM (2004) Hyaluronan participates in the epidermal response to disruption of the permeability barrier in vivo. Am J Pathol 165:1331–1341

Mullegger J, Rustom A, Kreil G, Gerdes HH, Lepperdinger G (2003) 'Piggy-back' transport of Xenopus hyaluronan synthase (XHAS1) via the secretory pathway to the plasma membrane. Biol Chem 384:175–182

Nishida Y, Knudson CB, Nietfeld JJ, Margulis A, Knudson W (1999) Antisense inhibition of hyaluronan synthase-2 in human articular chondrocytes inhibits proteoglycan retention and matrix assembly. J Biol Chem 274:21893–22189

Nykopp TK, Rilla K, Sironen R, Tammi MI, Tammi RH, Hämäläinen K, Heikkinen AM, Komulainen M, Kosma VM, Anttila M (2009) Expression of hyaluronan synthases (HAS1-3) and hyaluronidases (HYAL1-2) in serous ovarian carcinomas: inverse correlation between HYAL1 and hyaluronan content. BMC Cancer 9:143

Nykopp TK, Rilla K, Tammi MI, Tammi RH, Sironen R, Hämäläinen K, Kosma VM, Heinonen S, Anttila M (2010) Hyaluronan synthases (HAS1-3) and hyaluronidases (HYAL1-2) in the accumulation of hyaluronan in endometrioid endometrial carcinoma. BMC Cancer 10:512

Ohno S, Tanimoto K, Fujimoto K, Ijuin C, Honda K, Tanaka N, Doi T, Nakahara M, Tanne K (2001) Molecular cloning of rabbit hyaluronic acid synthases and their expression patterns in synovial membrane and articular cartilage. Biochim Biophys Acta 1520:71–78

Parkkinen JJ, Hakkinen TP, Savolainen S, Wang C, Tammi R, Ågren UM, Lammi MJ, Arokoski J, Helminen HJ, Tammi MI (1996) Distribution of hyaluronan in articular cartilage as probed by a biotinylated binding region of aggrecan. Histochem Cell Biol 105:187–194

Pasonen-Seppänen S, Karvinen S, Törrönen K, Hyttinen JM, Jokela T, Lammi MJ, Tammi MI, Tammi R (2003) EGF upregulates,

whereas TGF-beta downregulates, the hyaluronan synthases Has2 and Has3 in organotypic keratinocyte cultures: correlations with epidermal proliferation and differentiation. J Invest Dermatol 120:1038–1044

Pienimäki JP, Rilla K, Fulop C, Sironen RK, Karvinen S, Pasonen S, Lammi MJ, Tammi R, Hascall VC, Tammi MI (2001) Epidermal growth factor activates hyaluronan synthase 2 in epidermal keratinocytes and increases pericellular and intracellular hyaluronan. J Biol Chem 276:20428–20435

Recklies AD, White C, Melching L, Roughley PJ (2001) Differential regulation and expression of hyaluronan synthases in human articular chondrocytes, synovial cells and osteosarcoma cells. Biochem J 354:17–24

Rilla K, Siiskonen H, Spicer AP, Hyttinen JM, Tammi MI, Tammi RH (2005) Plasma membrane residence of hyaluronan synthase is coupled to its enzymatic activity. J Biol Chem 280:31890–31897

Rilla K, Oikari S, Jokela TA, Hyttinen JM, Kärnä R, Tammi RH, Tammi MI (2013) Hyaluronan synthase 1 (HAS1) requires higher cellular UDP-GlcNAc concentration than HAS2 and HAS3. J Biol Chem 288:5973–5983

Spicer AP, McDonald JA (1998) Characterization and molecular evolution of a vertebrate hyaluronan synthase gene family. J Biol Chem 273:1923–1932

Spicer AP, Nguyen TK (1999) Mammalian hyaluronan synthases: investigation of functional relationships in vivo. Biochem Soc Trans 27:109–115

Suzuki K, Yamamoto T, Usui T, Heldin P, Yamashita H (2003) Expression of hyaluronan synthase in intraocular proliferative diseases: regulation of expression in human vascular endothelial cells by transforming growth factor-beta. Jpn J Ophthalmol 47:557–564

Tammi R, Ågren UM, Tuhkanen AL, Tammi M (1994) Hyaluronan metabolism in skin. Prog Histochem Cytochem 29:1–81

Tammi R, Pasonen-Seppänen S, Kolehmainen E, Tammi M (2005) Hyaluronan synthase induction and hyaluronan accumulation in mouse epidermis following skin injury. J Invest Dermatol 124:898–905

Tammi RH, Passi AG, Rilla K, Karousou E, Vigetti D, Makkonen K, Tammi MI (2011) Transcriptional and post-translational regulation of hyaluronan synthesis. FEBS J 278:1419–1428

Tien JY, Spicer AP (2005) Three vertebrate hyaluronan synthases are expressed during mouse development in distinct spatial and temporal patterns. Dev Dyn 233:130–141

Vigetti D, Clerici M, Deleonibus S, Karousou E, Viola M, Moretto P, Heldin P, Hascall VC, De Luca G, Passi A (2011) Hyaluronan synthesis is inhibited by adenosine monophosphate-activated protein kinase through the regulation of HAS2 activity in human aortic smooth muscle cells. J Biol Chem 286:7917–7924

Vigetti D, Deleonibus S, Moretto P, Karousou E, Viola M, Bartolini B, Hascall VC, Tammi M, De Luca G, Passi A (2012) Role of UDP-N-Acetylglucosamine (GlcNAc) and O-GlcNAcylation of hyaluronan synthase 2 in the control of chondroitin sulfate and hyaluronan synthesis. J Biol Chem 287:35544–35555

Wang C, Tammi M, Tammi R (1992) Distribution of hyaluronan and its CD44 receptor in the epithelia of human skin appendages. Histochemistry 98:105–112

Weigel PH, Hascall VC, Tammi M (1997) Hyaluronan synthases. J Biol Chem 272:13997–14000

Weinbaum S, Tarbell JM, Damiano ER (2007) The structure and function of the endothelial glycocalyx layer. Annu Rev Biomed Eng 9:121–167

Wilkinson TS, Bressler SL, Evanko SP, Braun KR, Wight TN (2006) Overexpression of hyaluronan synthases alters vascular smooth muscle cell phenotype and promotes monocyte adhesion. J Cell Physiol 206:378–385

Yamada Y, Itano N, Hata K, Ueda M, Kimata K (2004) Differential regulation by IL-1beta and EGF of expression of three different hyaluronan synthases in oral mucosal epithelial cells and fibroblasts and dermal fibroblasts: quantitative analysis using real-time RT-PCR. J Invest Dermatol 122:631–639

Yoshida M, Itano N, Yamada Y, Kimata K (2000) In vitro synthesis of hyaluronan by a single protein derived from mouse HAS1 gene and characterization of amino acid residues essential for the activity. J Biol Chem 275:497–506